

**Efficacy of ELP as an Intratumoral Depot for Radionuclide Therapy of  
PC-3 Prostate Cancer in an Orthotopic, Nude Mouse Model**

by

Jeff Schaal

Department of Biomedical Engineering  
Duke University

Date: March 30, 2012

Approved:

---

Ashutosh Chilkoti, Supervisor

---

Wenge Liu

---

Mark Dewhirst

Thesis submitted in partial fulfillment of  
the requirements for the degree of Master of Science in the Department of  
Biomedical Engineering in the Graduate School  
of Duke University

2012

ABSTRACT

**Efficacy of ELP as an Intratumoral Depot for Radionuclide Therapy of  
PC-3 Prostate Cancer in an Orthotopic, Nude Mouse Model**

by

Jeff Schaal

Department of Biomedical Engineering  
Duke University

Date: March 30, 2012

Approved:

---

Ashutosh Chilkoti, Supervisor

---

Wenge Liu

---

Mark Dewhirst

An abstract of a thesis submitted in partial fulfillment of the requirements for the degree of Masters of Science in the Department of Biomedical Engineering in the Graduate School of Duke University

2012

Copyright by  
Jeffrey Laurence Schaal  
2012

## Abstract

Brachytherapy has emerged as one of the pre-eminent radiotherapy modalities for the treatment of prostate cancer. Current clinical methods utilize titanium encased radioactive seeds that are fixated within the prostate and permanently implanted. A novel brachytherapy alternative that has been developed to improve the delivery of radionuclide intratumorally is the synthetically designed elastin-like polypeptide (ELP). ELP can be injected in fluid form and undergoes an inverse phase transition to a biocompatible coacervate capable of serving as a biocompatible, intratumoral depot. Utilizing a previously developed ELP with a 7 tyrosine C-terminus tail, the therapeutic efficacy of ELP as a radioactive depot for treating prostate cancer was examined in a preclinical, orthotopic model. The orthotopic prostate model was first established by xenografting Bioware® PC-3M-luc-C6 cells into immunoincompetent, Balb/c nude mice. A non-invasive method for tracking tumor progression *in vivo* was developed using a correlation model comparing quantitative luminescent flux emitted from the cell line against the actual tumor size. The correlation between flux and tumor volume was determined to as  $Volume = 7.234 \times 10^{-9} x - 18.54$ , ( $\pm 21.7\%$ ), where  $x$  is the supine photon flux measured from a 10 second exposure taken 18 minutes after D-luciferin injection. Radionuclide conjugation of  $^{131}\text{I}$  to ELP was conducted using the established IODO-GEN reaction methodology and mice were administered a therapeutic dose of 2mCi / 40 $\mu$ l ELP / 150 mm<sup>3</sup> prostate tumor. Intratumoral deposition resulted in tumor regression in 90.9% of treated mice (n=11); 63.6% of which achieved tumor size reduction by over 60%. Radioactivity measurements demonstrate an 89.9% ELP depot retention over 2 weeks. Survival rates of the test group (64%) compared with controls (100%, n=14) indicate further testing is required to optimize radionuclide dosimetry.

# Contents

Abstract .....	iv
List of Tables .....	vii
List of Figures .....	viii
1. Introduction .....	1
1.1. <i>Prostate Cancer</i> .....	1
1.2. <i>Elastin-like Polypeptides</i> .....	3
1.3. <i>The Orthotopic Murine Model for Prostate Cancer</i> .....	6
1.4. <i>Experimental Purpose</i> .....	8
2. Materials and Methods .....	9
2.1. <i>Materials</i> .....	9
2.2. <i>Cell Culturing &amp; Collection</i> .....	9
2.3. <i>Orthotopic Prostate Inoculation Surgery</i> .....	10
2.4. <i>Bioluminescent Tumor Imaging</i> .....	12
2.5. <i>Establishing the Orthotopic Tumor Growth Model</i> .....	13
2.6. <i>ELP Construction and Purification</i> .....	14
2.7. <i>Radiolabeling Conjugation and Purification</i> .....	16
2.8. <i>Radiotherapy Administration and Monitoring</i> .....	18
3. Results .....	21
3.1. <i>Orthotopic Tumor Growth Model</i> .....	21
3.2. <i>ELP Construction and <sup>131</sup>I Radiolabeling</i> .....	27

3.3. <i>Radiotherapy Trials</i> .....	29
4. Discussion .....	33
4.1. <i>Orthotopic Tumor Growth Model</i> .....	33
4.2. <i>Radiotherapy Trials</i> .....	35
5. Conclusions .....	38
Appendix A : (VPGVG) <sub>120</sub> -Y <sub>7</sub> Design by Liu et al. ....	39
Appendix B : Orthotopic PC-3 Growth Model Data .....	42
Appendix C : Orthotopic Flux Correlation Data.....	43
References.....	44

## List of Tables

Table 1: Spin-purification recovery for different ELP concentrations .....	28
Table 2: ELP injection volumes and radioactive doses administered during radiotherapy .....	30
Table 3: Activity Information for Clinically Accepted Beta-Emission Radioisotopes.....	37
Table 4: Individual tumor sizes, both in terms of mass and volume, for mice inoculated with $1 \times 10^6$ PC-3 cells and grown for a pre-determined number of days .....	42
Table 5: Luminescent flux measurements for sacrificed mice, measured in different postures, and the corresponding tumor size .....	43

## List of Figures

Figure 1: <i>In vivo</i> bioluminescent intensity as a function of time elapsed after injection of 24mg/ml D-luciferin.....	21
Figure 2: Recorded prostate tumor sizes for Balb/C nude mice (n=34) after orthotopic inoculation with $1 \times 10^6$ PC-3M-luc-C6 cells. ....	23
Figure 3: Xenogen <sup>TM</sup> IVIS <i>in vivo</i> images comparing the PC-3M-luc-C6 photon flux intensity of different mice in both the prone and supine position. Each mouse was imaged at the designated time point and then sacrificed. ....	24
Figure 4: Luminescent photon fluxes for n=34 mice sacrificed at different time points after inoculation with $1 \times 10^6$ PC-3M-luc-C6 cells. ....	24
Figure 5: Correlation model for tumor mass as determined from luciferase luminescence measured in the supine position. ....	26
Figure 6: Correlation between luciferase luminescence measured in the prone position and actual tumor mass. ....	26
Figure 7: Model depicting the dependency of PC-3 tumor volume on its measurable mass. ....	27
Figure 8: Transition temperatures for E <sub>4</sub> 120-7Y prepared at different concentrations.....	28
Figure 9: Intratumoral radiation level measured over time and compared against the theoretical decay behavior for <sup>131</sup> I. ....	31
Figure 10: Tumor regression in mice resulting from intratumoral radiotherapy .....	31
Figure 11: Survival chart comparing mice having received radiotherapy (n=12) against those that received control injections of unlabeled E <sub>4</sub> 120-7Y (n=14).....	32
Figure 12: (A) Turbidity profile displaying the phase transition profile for ELP molecules (containing a V residue) varying in pentapeptide repeat length. (B) Percent of ELP depot retained intratumorally over time. ....	39
Figure 13: (A) Transition temperature of ELP (VPGVG) <sub>120</sub> as determined over varying concentrations by measuring relative absorbance at 350nm. (B) 1-week intratumoral retention performance of ELP depots formulated at varying concentrations.....	40

Figure 14: (A) Transition temperatures of the ELP construct (VPGVG)<sub>120</sub> @ 1000 μM with varying number of carboxyl-terminus tyrosine residues. (B) Intratumoral retention performance of varying tyrosine tail lengths. .... 41

# 1. Introduction

## 1.1. *Prostate Cancer*

Prostate cancer is the single most common cancer afflicting men in the United States and the second most common cancer worldwide [1]. Moreover, it is the 2<sup>nd</sup> leading cause of cancer related death for males in the United States. An exocrine gland within the male reproductive system, the prostate is responsible for alkalizing semen to improve its survival life [2]. Healthy prostate tissue is characterized by an epithelium containing luminal epithelial cells, basal cells and neuroendocrine cells. As men reach their mid-forties, these cells naturally undergo a period of heightened proliferation known as benign hyperplasia [3]. This growth can continue unabated, however, leading to the development of prostatic adenocarcinomas that are characterized by the absence of basal cells in the epithelium, glandular formation, luminal differentiation and proliferation of malignant tumor cells. As the prostate adenocarcinomas mature, the tumor cells often exhibit a change in phenotypic expression. Early stage carcinomas are slow growing and cells express both androgen receptors (AR) and prostate-specific antigen (PSA). As they progress, tumor cells become more aggressive and enter a state of hormonal independence whereby AR and PSA are not expressed [4]. Men who contract prostate cancer typically exhibit symptoms that include urinary incontinence, urinary inflammation, sexual dysfunction, back pain, loss of weight and pain in the extremities.

The traditional clinical methods for treating prostate cancer have included either exposing a patient to external beam radiation or surgically performing a prostatectomy. Both methods have proven effective, but contain several drawbacks. Multiple surgical techniques exist depending on that advancement of the prostate tumor with the most invasive being radical prostatectomy. In most cases, the inherent surgical trauma requires patient hospitalization for 2-4 days after the operation and catheterization for a week or two. The success of the surgery is

individually dependent on the surgeon's skill with a high chance of recurrence if the tumor is not completely removed. External beam radiation offers a non-invasive and effective method for killing the malignant cells in the prostate region. Unfortunately, it also causes radiation damage to the skin and surrounding tissues that exist along its penetration path. This modality enhances the ability to kill all tumor cells, but often afflicts healthy tissue in addition. Over the past 2 decades, fortunately, a new form of prostate cancer radiotherapy has found clinical adoption: brachytherapy.

Brachytherapy is the term for when the radioactive source is placed near or in the tumor site, thereby capitalizing on the tumor killing efficacy of radiation while minimizing damage peripheral tissues. The proximal placement of the radioactive source at the site of treatment allows lower levels of radiation to be administered while achieving the same efficacy. Modern prostate cancer brachytherapy involves the injection of either  $^{125}\text{I}$  or  $^{103}\text{Pd}$  radioactive isotopes encapsulated within titanium seeds into the prostate. The seeds are spatially orientated to achieve a homogenous radiodosimetry profile throughout the prostate tumor. The titanium casing renders the seeds biologically inert and causes fibrous encapsulation within the prostate. The lower radioactivity and spatial mapping of the dosimetry profile ensure minimal radiation penetration to other organs. Light irradiation of the urethra and rectum typically leads to minor symptoms including urinary irritation and ejaculation discomfort. The simplicity of the procedure enables an outpatient procedure of typically 45 minutes while achieving complete tumor remission in 81% of patients characterized with intermediate to low risk cancer, similar to both radical prostatectomy and EBRT [5].

The major disadvantages from the use of titanium encapsulated seeds in brachytherapy seeds arises from the fact that implants are spatially fixed during treatment and permanent. Careful pre-planning and algorithmic mapping ensures that seeds are optimized spatially within

the original tumor. As the isotopes decay, however, the radiation penetration profile throughout the tumor tissue may become non-homogenous. In addition, as the tumor recedes due to treatment, the seeds fixed at the boundary can heighten peripheral tissue irradiation or even ‘tumble’ out of the prostate. The permanent presence of the metal seeds in the healed prostate has also been known to induce long term urinary and sexual discomfort in some patients [6]. Finally, the general procedure for ensuring correct spatial placement of the seeds *in situ* is technically complicated and prone to error. Establishing an alternative method that simplifies the procedure and reduces the room for error would greatly improve brachytherapy administration.

The short procedural times, quick recovery, reduced side effects and clinical success achieved with brachytherapy has quickly made it a popular procedure for treating prostate cancer. The current drawbacks of titanium encapsulated seeds have led researchers to investigate the possibility of developing a protein conjugate for the delivery of intratumoral radionuclides. To provide a value-add alternative to existing brachytherapy, such a protein must be biocompatible, be capable of radionuclide conjugation, and remain biochemically stable over the course of the radiotherapy while being capable of non-toxic degradation over a longer period of time. One molecule that has shown promise in meeting such design criteria is the synthetically designed elastin-like polypeptides (ELP).

## **1.2. *Elastin-like Polypeptides***

Elastin-like polypeptides, or ELP molecules, are a class of recombinant biopolymers that exhibit an inverse phase transition response to thermal stimuli [7]. ELP are synthetically constructed proteins consisting of the pentapeptide sequence of  $(VPGXG)_n$ , where X can be any ‘guest’ amino acid. This native structure causes ELP molecules to be inherently hydrophobic. At lower temperatures, ELPs are typically soluble due to the low thermodynamic energy of their

solvent system. At high temperatures, however, they transition to a packed coacervate phase that maximizes the entropic energy of the overall system. This inverse phase transition is triggered sharply once the aqueous solution achieves a specific temperature ( $T_t$ ), known as a lower critical solution temperature or transition temperature.

By taking advantage of this unique thermal property of ELP, it is then possible to construct a polymeric delivery construct that can be injected in liquid form intratumorally, whereby it would immediately transition into a solid depot at body temperature. Intratumoral delivery of an ELP radio-conjugate is particularly attractive because it circumvents the difficulty of tumor penetration in systemic drug delivery [8]. Direct injection simultaneously achieves delivery of the radio dose into the center of the tumor, limits exposure to other tissues, and concentrates the effective dose for maximal effect. Direct injection of ELP in its initial liquid phase allows molecules to diffuse throughout the tumor interstitial space, enabling a uniform radiodose delivery throughout the tumor. Synthetic ELP variants have also been shown to be both biocompatible and non-toxic since their similarity to natural occurring elastin renders them indistinguishable to the immune system [9]. Likewise, their natural amino acid composition ensures that they are biodegradable into biocompatible monomers [10]. The fact that ELP is cheaply grown from *E. coli* bacterial cultures in high yields and can be purified using a batch, inverse-transition cycling procedure also make it very attractive for production.

In order to successfully serve as an intratumoral depot, however, the properties of the ELP molecule design must first be modified to achieved a  $T_t$  that is well under the physiological body temperature of 28°C [8]. The specific transition temperature of a construct has been found to vary depending on several different properties, thus providing several means for tuning ELP characteristics for use as an intratumoral depot. First, the guest residue insert, X, in the ELP sequence greatly impacts the overall polymeric behavior due to its hydrophobic contributions and

side chain functional groups. Hydrophobic amino acid inserts serve to lower the  $T_t$ . Functional groups, such as the thiol group in cysteine, can lead to cross-linking of polymeric molecules which also affect the overall  $T_t$ . A second property that is inherent in the molecular design is the attachment of ELP to carboxyl-terminus tail residues or fusion proteins. The relative hydrophobicity of the attachment can again contribute to the overall hydrophobic nature of the construct, driving changes in the  $T_t$ . The third factor that contributes to the  $T_t$  is the inherent entropy and polarity of the solvent used for suspension. Fourth, it has been demonstrated that increasing the concentration of an ELP construct will also lower the transition temperature. Finally, by increasing the number of pentapeptide repeats, thus increasing the overall molecular weight of the molecule, will also lower the transition temperature.

In a previous study performed by Liu et al. [11], an ELP molecule was designed and optimized for use as a radionuclide, intratumoral depot in a subcutaneous murine model. This ELP, E<sub>4</sub>120-7Y, was designed using a valine guest residue, consisting of 120 repeats, and having a 7 tyrosine carboxyl-terminus tail, (VPBVG)<sub>120</sub>-Y<sub>7</sub>, suspended in PBS and administered at a concentration of 1000  $\mu$ M. In their trials, VPGVG was selected as the pentapeptide sequence due to it being previously well characterized *in vivo* and having transition temperature in the appropriate physiological range, 20-30°C. Further experiments, as referenced in Appendix A, were conducted to determine the relative importance of molecular weight, concentration and number of tyrosine residues on the both the transition temperature and intratumoral depot. A threshold of 50 kDa (120 repeats) was found to maximize intratumoral retention at 60% over 1 week while maintaining the proper physiological transition temperature. The concentration of 1000  $\mu$ M improved the retention further while lowering the  $T_t$  down to ~23°C. Finally, addition of the c-terminus tyrosine residues further heightened tumor retention up to 85% over 2 weeks and reduced the  $T_t$  to ~21.5°C [11].

For their proof of concept experiment, Liu et al. used ELP as a  $^{131}\text{I}$  intratumoral depot that was injected into tumor lines xenografted subcutaneously on the murine dorsal flank. The therapeutic regimen called for injection doses of 2 mCi / 40  $\mu\text{l}$  ELP / 150  $\text{mm}^3$  tumor deposited at the central core of the tumor. Their results demonstrated complete tumor remission in 72% of the animals with a survival rate of 93%. While their findings were promising, the subcutaneous model employed does not properly model the histological, biochemical and anatomical settings of the prostate. In order to fully assess ELP's radiodepot potential, further work must be conducted to test the efficacy of ELP for tumors grown in the prostate organ itself. Constructing and evaluating the therapeutic efficacy in an orthotopic model would provide important information about the relative sensitivity and degradation characteristics of the ELP depot in an environment homologous to the human prostate.

### ***1.3. The Orthotopic Murine Model for Prostate Cancer***

To properly evaluate ELP as a radiotherapeutic depot for potential clinical application, further testing was required that would examine its efficacy and safety when injected into the prostate itself. Unlike the subcutaneous model, an orthotopic model examines therapeutic effectiveness in an environment that is histologically and biochemically equivalent to clinical application. While mice prostates are anatomically dissimilar from human prostates in the fact that they are multi-lobed, it has been characterized that dorsolateral lobe of the mouse is histologically and biochemically similar human prostate carcinoma [12]. Thus, establishing an orthotopic mouse model could provide very important insight into the potential efficacy of using ELP as an intratumoral.

Two main factors were considered for constructing an effective orthotopic animal model. First, clinical efficacy is more easily determined when animal experiments are conducted with

human cancer lines are xenografted into the animal and assessed against a particularly therapeutic strategy. As the mouse immune system will typically reject injected human cells, this requires a special type of mouse. For this purpose, out-bred Balb/C nude mice were purchased from Duke University's Cancer Center Isolation Center / Immunoincompetent Rodent and Biohazard Facility (CCIF/IRBF). Balb/C nude mice have been irradiated to remove their thymus gland, producing a strain of immunodeficient mice ideally suited for conducting human cell carcinoma xenografting.

The second important factor that determines how the animal model is constructed is the need to enable a non-invasive means for tracking prostatic tumor size *in vivo*. Tumor progression tracking is important for determining the correct therapeutic dosage a mouse should be administered and for tracking tumor regression after such a treatment. Unlike subcutaneous models, where the tumor is readily measured via calipers, an orthotopic prostate model is completely recessed. Because of this, an imaging method is required that can non-invasively determine the tumor size. This was achieved by carefully selecting a specific prostate tumor cell for xenografting: the Bioware® cell line PC-3M-luc-C6 from Caliper Life Sciences.

The Bioware® cell line PC-3M-luc-C6 is a stable bioluminescent prostatic tumor line derived from a PC-3 human adenocarcinoma that has been transfected with the North American Firefly luciferase gene. PC-3 is a well-characterized and commonly used cell line in prostate cancer research. It is an aggressive form of clinical prostate cancer known to lack androgen receptors and also does not display prostate specific antigen (PSA) [13]. Because its growth is both aggressive and independent of the human hormone androgen, the PC-3 cell line is ideal for xenografting a human tumor into mouse models. Moreover, expression of the luciferase enzyme within the tumor cells enable the catalytic conversion of luciferin, in the presence of ATP and oxygen, to oxyluciferase which results in emission of light (150-250 photons/sec/cell) [14]. This genetic alteration of the cell line results in a cellular bioluminescence that can be observed upon

administration of D- luciferin. This luminescent signal should increase proportionally with the number of cells present in each tumor and can be quantitatively measured using commercially available imaging equipment.

#### ***1.4. Experimental Purpose***

This study served two purposes. First, it sought to develop a clinically relevant prostate model for preclinical trials that enabled a non-invasive means for accurately tracking tumor growth. It was hypothesized that xenografting the luciferase expressing PC-3M-luc-C6 cells orthotopically into the dorsolateral prostate lobe of immunoincompetent mice would accomplish this goal. Second, the preclinical trials examined the efficacy administering the previously formulated ELP as an injectable polymer capable of forming a stable coacervate depot for delivering intratumoral radiotherapy. It was hypothesized that the <sup>131</sup>I-ELP depot would provide a biocompatible, non-toxic brachytherapy alternative for achieving tumor regression and eventual remission in the test subjects.

## **2. Materials and Methods**

### **2.1. Materials**

Bioware® PC-3M-luc-C6 cells were purchased from Caliper Life Science. All Balb/C nude mice were obtained through Duke University's Cancer Cell Isolation Facility / Immunoincompetent Rodent and Biohazard Facility (CCIF/IRBF). Gibco minimum essential media (MEM #11095), Earle's salts, L-glutamine, sodium pyruvate, non-essential amino acids, fetal bovine serum, penicillin/streptomycin, Dulbecco's modified Eagle's medium (DMEM), Gibco PBS, endotoxin tested water and trypsin were purchased from Invitrogen through Duke University Cell Culture Facility. D-luciferin potassium salt was acquired from Gold Biotechnology. Stock of isoflurane was purchased through Baxter International Inc. Terrific Broth® (TB Dry®) powder growth media was purchased from MO BIO Laboratories. Gibco® kanamycin sulfate was purchased from Invitrogen. Kanamycin resistant *E. coli* cells transfected with the gene for E<sub>4</sub>120-7Y and were obtained from frozen stock through the Chilkoti lab at Duke University. Detoxi-Gel™, 40 kDa Desalt spin columns, and Pierce® IODO-GEN Pre-Coated iodination tubes were purchased from Thermo Scientific. <sup>131</sup>I was procured from Perkin Elmer through the Duke Medical Center Radiopharmacy.

### **2.2. Cell Culturing & Collection**

The medium used for culturing PC-3M-luc-C6 cells was made from a mixture of 87% Gibco MEM #11095 (containing Earle's salts and L-glutamine), 10% fetal bovine serum, 1% sodium pyruvate, 1% non-essential amino acids and 1% penicillin / streptomycin vacuum filtrated through a Corning system cellulose acetate membrane and stored at 4°C. The PC-3 cells were cultured as monolayers on Corning culturing flasks with media (at a 15 ml per 75 cm<sup>2</sup> flask area)

inside a cell incubator maintained at 37°C with a 5% CO<sub>2</sub> gas supply. Cell cultures were allowed to grow until reaching 80% confluence and then split off into new culture flasks.

For cell collection, all procedures were carried out in a sterilized biological hood. The old media was initially suctioned out of the flask and then the confluent cells were gently washed in 5 ml of PBS. 0.05% trypsin-EDTA was added to the culture flask until the entire culture surface was slightly covered and incubated for 3 more minutes. After allowing time for the trypsin to cleave the cells adhering to the flask surface, media containing 10% FBS is added into the flask at a 2:1 volume ratio of the trypsin and gently mixed, inactivating the trypsin enzyme. The entire solution was then transferred to a centrifuge tube and centrifuged at 1200rpm for 3 minutes. The cells were spun down, the supernatant removed and the cell pellet resuspended in 1 ml of DMEM.

The cell count was then determined by mixing 10 µl of the resuspension with 20 µl of trypan blue stain. 10 µl of the stained cells were placed on a hemocytometer and viable cells were counted under light microscopy. The total number of collected cells were then determined from the counted sample density. When the total count of cells is known, they are centrifuged again at 1200rpm for 3 minutes and the supernatant removed. The cell pellet is then resuspended in DMEM to bring at a volume to bring the total concentration of cells to 1x10<sup>6</sup> PC-3 cells per 10 µl.

### ***2.3. Orthotopic Prostate Inoculation Surgery***

Prior to surgery, all surgical equipment and the rodent surgical board were sterilized using an hour long gravity cycle in an autoclave. Anesthesia was prepared by mixing 0.3 ml of ketamine with 0.04ml xylazine and 0.66 ml of 0.9% saline solution. PC-3M-luc-C6 cells were cultured and collected according to the previously described method to ensure an inoculation

concentration of  $1 \times 10^6$  cells per 10  $\mu$ l of DMEM and then placed on ice. Balb/C nude mice approximately 6-7 weeks old were ordered from the Immunoincompetent Rodent and Biohazard Facility and housed in the Cancer Center Isolation Facility (CCIF) at Duke University.

The surgical procedure was carried out within the CCIF. The surgical area was set up in a sterilized hood. In the surgical area, the rodent surgery board was placed on top of a heating pad to maintain each animal's body temperature while anesthetized. Similarly, a staging area was set up with a second heating pad for animal prep and resting. Prior to the procedure, each mouse was weighed and labeled. Labeling was determined according to the batch number and a specific mouse number. The specific mouse number was tracked by the relative position of punching a hole in each mouse's ear. Anesthesia was administered via *intra-peritoneal (i.p.)* injection to each mouse at a dosage of 60  $\mu$ l ketamine / xylazine per 20 g of body weight. Upon losing motor control, the mice were moved to the staging area and were sanitized by wiping down the incision area first with soap, then twice with ethanol. They were then allowed to sit for 10-15 minutes until reach the surgical plane of anesthesia which was verified by performing the pinch test on the animal's hind leg.

Once fully anesthetized, the mouse was fixed in the supine position on the rodent surgical board and covered with surgical paper. Using surgical scissors, a 1 cm midline incision was then performed into the lower abdominal skin. The peritoneal cavity membrane was then tented, massaged to ensure no additional organs were lifted, and then opened with a similar 1 cm incision. Using tweezers, the bladder was gently located and raised out of the peritoneal cavity until the prostate was visible. The prostate was then fixed using rounded tweezers for easy inoculation. The PC-3 cells were taken off ice, mixed and loaded into a 30 gauge syringe. The syringe was then inserted into the right dorsolateral lobe of the mouse's prostate and injected with 10  $\mu$ l of cell solution. A cotton swab was placed at the site of injection and the syringe needle

slowly withdrawn; using the swab to blot and soak up any potential backflow. The prostate and bladder were then recessed back inside the peritoneal cavity. The membrane was closed using the purse-string technique with a 5-0 absorbable suture. The skin was then closed using a series of 4-5 evenly spaced, interrupted stitches.

After completion of surgery, each mouse was moved to the resting area to recover. Triple antibiotic ointment was applied to the surgical incision wound and given a sub-cutaneous injection of buprenorphine for pain relief at a dose of 0.05-0.10 mg per kg of mouse body weight. Additional eye lubricant was applied as necessary. The mice were allowed to regain consciousness before being returned to their cages. Each mouse was monitored for 2-3 days following the procedure to ensure no complications, such as excessive weight loss or post-surgical infection, occurred.

#### **2.4. Bioluminescent Tumor Imaging**

Luciferin imaging solution was prepared from mixing D-luciferin potassium salt with double distilled PBS solution at a mixture of 24 mg/ml and then filter sterilized using a 0.2  $\mu$ m filter. Prepared solution was wrapped in aluminum foil and stored at -80°C to maintain luminescent stability. Tumor imaging was conducted using the Xenogen<sup>TM</sup> IVIS 100 imaging system from Caliper Life Sciences. Mice were first measured to determine their body weight. Next, they were anesthetized using isoflurane and then placed into the imaging chamber. Control images were then taken measuring the bioluminescent photon flux for an exposure time of 10 seconds at a subject height of 1.5cm. The mice were administered an *i.p.* injection of luciferin, at a dosage of 100  $\mu$ l / 16 grams of body weight, and placed back into the IVIS imaging chamber with their noses in isoflurane outlets. Luminescence was then measured by acquiring 10 second exposure images of the total photon flux being emitted from the mouse tumor cells.

Initial experimental trials were conducted to determine the time elapsed post-injection at which the tumor cells exhibit maximum luminescent intensity. 4 mice were injected with luciferin and independently imaged at time points of 5, 10, 12.5, 15, 17.5, 20, 25, 30, 35, 40, 45 and 50 minutes. Images were taken measuring the total photon flux measured from a 10 second exposure over the mouse's body from the neck down. Intensity was then plotted versus time and an optimal, peak time determined.

## ***2.5. Establishing the Orthotopic Tumor Growth Model***

To establish an *in vivo*, orthotopic growth model for the PC-3 tumors, 30 Balb/c nude mice were inoculated with  $1 \times 10^6$  PC-3M-luc-C6 cells. The tumors were allowed to grow within each of the mice for a predetermined number of days (10, 14, 16, 18, 21, 23, 27, and 30 days) in sets of 3-4 mice per time point. Upon reaching the targeted day, the designated mice were first imaged following the IVIS/luciferin method described previously. To determine the most accurate method of imaging, the mice were imaged in the prone position 15 minutes post-injection and in the supine position 18 minutes post-injection. In order to understand the threshold of luminescent reflectivity limits, control mice inoculated with tumor cells but lacking luciferin were imaged next to a test mouse injected with luciferin. The relative reflective flux on the secondary mouse was then imaged in both the supine and prone position.

Next, the mouse was sacrificed via cervical dislocation (while under anesthesia), followed by secondary bilateral thoracotomy. The tumor was then excised from the peritoneal cavity, making sure to carefully dissect all portions of the tumor. After 40 minutes, the excised tumor and the dissected mouse with its peritoneal cavity organs exposed were placed within the IVIS chamber and imaged. The dissected mouse is included so as to determine the presence of any residual tumor cells that were not successfully excised. Finally, the weight and dimensions

of the excised tumor were measured to determine its actual size. To ensure that the model only includes data where the measured tumor size (volume and mass) is completely responsible for the *in vivo* luminescent signal, data was only included for correlation if the residual luminescent signal was less than the previously determined reflectivity threshold. Correlation models for volume, mass, supine flux, prone flux and *ex vivo* flux were then established and evaluated.

## **2.6. ELP Construction and Purification**

A starter culture was prepared by mixing 2.7 grams of TB Dry® in 50 ml of H<sub>2</sub>O in an Erlenmeyer flask and then autoclaved. Kanamycin sulfate was dissolved in ddH<sub>2</sub>O at a 10mg/ml ratio and sterile filtered. 50µl of kanamycin solution was then added to the starter flask media. *E. coli* cells capable of expressing the ELP protein E4120-7Y were obtained from a previously established stock of frozen cells that had been stored in 7% DMSO in dd-H<sub>2</sub>O at -80°C and added to the starter flask. The cells were then amplified overnight at 37°C in an incubating shaker. Simultaneously, twelve Erlenmeyer flasks were prepared with 55 grams of TB Dry® mixed in 1 liter of H<sub>2</sub>O and then autoclaved. The following day, 1 ml of kanamycin solution was added to each liter flask. The starter flask was retrieved from the incubator and the contents centrifuged at 3000 rpm and ~4°C for 15 minutes. The supernatant was discarded; then the cells were re-suspended in sterilized TB media and split evenly amongst the 1 liter Erlenmeyer flasks. The flasks were then placed in the shaking incubator and amplified for 24 hours at 37°C and 190 rpm.

The following day, the culture broth from each flask was centrifuged down at 3000 rpm and 4°C for 15 minutes and the supernatant discarded. The cell pellet was then re-suspended in 10 ml of chilled PBS. The suspension was then sonicated on ice using a cycling method of 10 seconds on, 40 seconds off for a total sonication ‘on’ time for 6-9 minutes. After the cells have been thoroughly lysed, 10% polyethyleneimine (weight by volume of ddH<sub>2</sub>O) was mixed into the

solution at a volume of 2ml for every 1liter flask cultured. The solution was transferred to centrifuge tubes and centrifuged at 13000rpm at 4°C for 15 minutes to separate the soluble ELP from the non-soluble cell membrane components.

Inverse transition cycling was then applied to further purify the ELP from other soluble proteins. For the first hot cycle, 0.5 mole of NaCl were added for each flask cultured to help transition ELP out of solution. The solution is additionally ‘hot spun’ at 13000 rpm and 37°C for 15 minutes to separate ELP into a coacervate phase. The supernatant is discarded and the pellet is re-suspended in 4 ml of chilled PBS while on ice. A cold spin is then conducted at 13000 rpm for 10 minutes to further remove non-soluble elements. The supernatant containing soluble ELP was transferred to new centrifuge tubes and underwent 3 additional hot spin / cold spin cycling. For these cycles, however, NaCl was not added to the solution to induce transitioning as thermal transitioning was sufficient to achieve ELP phase purification. After the 4<sup>th</sup> hot spin, the ELP should be re-suspended in chilled, endotoxin free dd-H<sub>2</sub>O. The 4<sup>th</sup> cold spin was then conducted per usual and the supernatant retained. The ELP solution is then dialyzed overnight in 5 liters of dd-H<sub>2</sub>O in a 4°C fridge.

Next, endotoxins must be removed from the ELP solution. Detoxi-Gel<sup>TM</sup> endotoxin removal gel was added into a 5ml spin column and allowed to sit for 30 minutes to create an endotoxin removal resin. The resin activity was then regenerated by flowing through 13 ml of 1% sodium deoxycholate (by weight) in endotoxin free H<sub>2</sub>O at room temperature. The resin was then washed 5 times at resin volume with PBS. The column was then capped and chilled on ice. 2 ml of ELP solution was added to the column, equilibrated for 30 minutes, and then allowed to run through the resin. The first run through was discarded. ELP solution was then similarly added to the removal column, equilibrated on ice for 30 minutes, and then allowed to run through gravitationally into a collection tube, purified of endotoxins.

After dialysis and endotoxin removal, the ELP solution was placed in 50 ml centrifuge tubes and frozen in the -80°C freezer for 2 hours. The tubes are then retrieved, masked in Kim-wipe tissue paper and lyophilized under vacuum at -80°C for 2 days to fully dehydrate the purified ELP. Stocks of E<sub>4</sub>120-7Y were then prepared by re-suspending the ELP for a final time in PBS. 500 μM E<sub>4</sub>120-7Y was prepared by mixing 25 mg of ELP in 1 ml of PBS, 750 μM was mixed at 37.5 mg/ml, 1000 μM was mixed at 50mg/ml, 1250 μM was mixed at 62.5 mg/ml, and 1500 μM as mixed at 75 mg/ml. Purity was verified by running a protein gel ladder. Finally, the transition temperature of each concentration was similarly verified by measuring absorbance while raising solution temperature from 15°C to 50°C at a rate of 1°C per minute using a Cary 300 Bio Spectrometer.

## ***2.7. Radiolabeling Conjugation and Purification***

Prior to radiolabeling, an additional set of trials were conducted to find the ideal size purification conditions to achieve maximal ELP recovery from the Desalt spin columns. Various concentrations of E<sub>4</sub>120-7Y were centrifuged under varied times and rpm speeds to determine the percent recovery. From the results, the concentration of E<sub>4</sub>120-7Y most suitable to radiolabeling was selected; along with the maximal yield settings that achieved size exclusion of ELP through the column.

Once fully purified, <sup>131</sup>I was conjugated to the ELP molecule through a well-characterized radiolabeling methodology. First, 40 kDa Desalt spin columns were prepared for later use. The columns were centrifuged for 3 minutes at 2500 rpm to remove the storage buffer. 1-2.5 ml of PBS were added to the column and similarly centrifuged to further cleanse the column of remaining buffer. In this case, the volume of PBS depended on the size of the column used. Experiments made use of both 5 ml and 2 ml spin columns, depending on the amount of

ELP to be labeled (the 5 ml column required a minimum ELP volume of 300  $\mu$ l to be effective). The column was then capped and stored with PBS directly on ice. The 500  $\mu$ M E<sub>4</sub>120 with 7 tyrosine molecules was also thawed, fully suspended, and then stored on ice.

All radiolabeling procedures were carried out in an approved lab under a precautionary, lead brick enclosed hood. All equipment necessary for handling the ELP was pre-chilled on ice to prevent thermal transition into its coacervate phase during processing. 50 mCi of the <sup>131</sup>I isotope were retrieved from the Duke Medical Center Radiopharmacy and measured for the actual radioactivity using a gamma detector. 10-15 mCi of <sup>131</sup>I were then added directly to the IODO-GEN catalyst coated bottom of the Pierce® precoated tubes. The individual radioactivity of each tube was then measured. Assuming a 75% radiolabeling efficiency factor ( $f_{label}$ ), the total amount of ELP required in each reaction tube was determined from the formula:

$$ELP_{req} = a_{131I} * f_{label} * \frac{40\mu l}{5mCi}$$

, whereby 5 mCi / 40 $\mu$ l is the targeted activity

concentration post reaction and  $a_{131I}$  is the measured activity within each tube. E<sub>4</sub>120-7Y was then added at the determined volume. The IODO-GEN catalyzed reaction was then allowed to proceed for 30 minutes, with gentle agitation every 5 minutes, while the tubes were kept on ice.

Upon completion of the conjugation, the reaction solution was completely collected and transferred to the prepared Desalt spin columns with clean collection tubes. The columns were then centrifuged at 2500 rpm for 4 minutes, while chilled to 4°C, to purify the ELP from any free iodine solution. The collected contents of labeled ELP were then transferred to a marked eppendorf tube. The spin column was returned to the ice for 10 minutes, and then centrifuged a second time to recover additional labeled ELP. All labeled ELP solution was then carefully measured to determine the exact volume and activity of the successfully radiolabeled E<sub>4</sub>120-7Y.

## **2.8. Radiotherapy Administration and Monitoring**

1 week prior to radiotherapy, mice received prophylactic supplements of KI dissolved in their drinking water (0.4 g / 100 ml H<sub>2</sub>O), preventing the potential uptake of <sup>131</sup>I by the thyroid by over saturation with non-radioactive iodine. On the day of the radiotherapy, each mouse targeted for therapy was imaged using the previously described luciferin bioluminescent method. The corresponding tumor size of each mouse was then calculated using the established correlation model.

On the day of radiotherapy, the radiolabeled E<sub>4</sub>120-7Y had to be first adjusted to the appropriate 1000 μM concentration before it could be administered to the mice. This was achieved by first adding unlabeled E<sub>4</sub>120 at 500μM to bring the activity concentration down to 4 mCi / 40μl. Next, the ELP was further mixed at a 1:1 ratio with unlabeled E<sub>4</sub>120 at 1500μM to achieve a final administration solution concentration of 1000μM E<sub>4</sub>120-7Y with the target activity of 2 mCi / 40 μl. The ELP was next loaded into a pre-cooled Hamilton 500μl microsyringe. The syringe was connected to a 6-8inch catheter with a beveled needle for injection. The entire syringe was attached to a motorized Hamilton infusion pump with a drive setting of 160 μl / min. The entire apparatus was then covered in ice packs to inhibit ELP transitioning.

For administering the radiotherapy, the same surgical preparation and incision procedures were followed. Mice were pre-weighed and received *i.p.* injections of 30% ketamine / 4% xylazine in accordance with their body weight. Upon achieving the surgical plane of anesthesia, they were fixed to a heated surgical board in the supine position. A 1 cm incision of the lower abdomen skin and peritoneal cavity membrane was used to expose the developed prostate tumor. The catheterized needle for injecting ELP was inserted into the tumor center of mass. The motorized Hamilton infusion pump was then used to intratumorally inject the predetermined

volume of radiolabeled ELP based on the therapeutic dose of 2 mCi / 40 $\mu$ l ELP / 150 mm<sup>3</sup> of tumor. Once infusion was complete, the catheter needle was held in place a further 15 seconds to ensure complete transition of the ELP coacervate. The needle was then removed and returned to ice.

The mouse peritoneum was surgically closed using a purse-string suture technique, while the skin was sutured using a line of interrupted single stitches. Mice were placed in the recovery area, administered triple antibiotic ointment and received a sub-cutaneous injection of buprenorphine for pain relief. Successful radiotherapeutic injection was confirmed by measuring the <sup>131</sup>I activity within the mouse using a gamma detector post-surgery. In addition to the radiotherapeutic treatments, 12 mice were also set up as controls and received intratumoral injections of unlabeled ELP at a concentration of 1000  $\mu$ M. The surgery and injections followed the same procedures as the radiotherapy mice in all other aspects. Upon recovery from the anesthesia, all mice were returned to their cages. To prevent excessive weight loss, following surgery and initial radiation exposure, mice were provided a supplementary diet of sterilized peanut butter in addition to their normal food. The cages were then shielded behind lead barriers to isolate other lab inhabitants from accidental radiation exposure.

During the first week following radiotherapy, the body weight and radioactivity of each mouse was checked daily. Each mouse was examined for post-surgical infection, urinary complications, and excessive weight loss. Tumor size was checked every 2 days using the luciferin imaging method. After the initial week, monitoring was reduced to checking body weight and radioactivity every other day while tumor imaging was reduced to twice a week. If at any time a mouse's body weight fell and remained beneath 85% of its pre-surgical weight, it was euthanized to prevent suffering. Similarly, if a tumor size was observed to grow above 700 mm<sup>3</sup>, the mouse was euthanized. Finally, if a mouse was observed to have a distended bladder or

undergo renal failure due to radioactivity damage to urinary organs, the mouse was euthanized.

All mice in the study were observed and monitored for a period of up to 60 days post-treatment.

### 3. Results

#### 3.1. Orthotopic Tumor Growth Model

The first step in constructing a bioluminescent model was to ascertain the duration of time necessary for luciferase activity to reach peak intensity. Since the relative abundance of luciferin injected intra-peritoneally into a mouse may affect how long a tumor can express the full extent of its enzymatic bioluminescence, determining the time of peak intensity is important for comparing different size tumors in across separate animals. Earlier animal trials leveraging luciferin imaging for subcutaneous tumor grafts (Chen, M. unpublished work from Duke University) found that 15 minutes were ideal luminescent imaging. Due to potential differences in luciferin diffusion and tumor accessibility characteristics in the orthotopic model, this parameter was reevaluated.

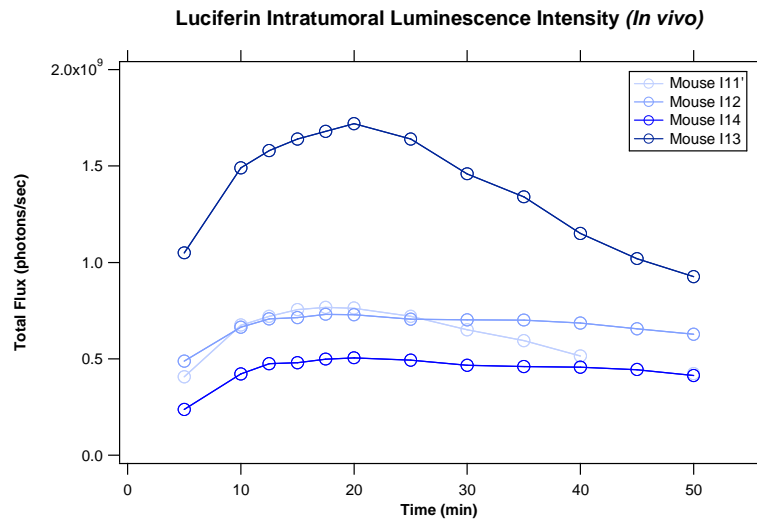


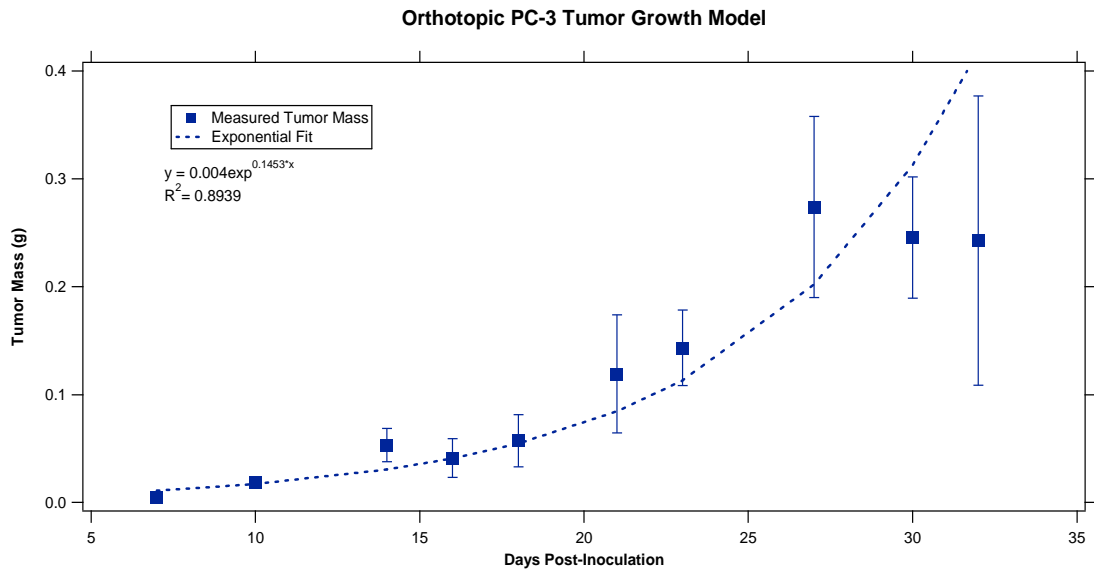
**Figure 1: *In vivo* bioluminescent intensity as a function of time elapsed after injection of 24mg/ml D-luciferin.**

As shown in Figure 1: *In vivo* bioluminescent intensity as a function of time elapsed after injection of 24mg/ml D-luciferin, the peak intensity was found to vary across the different mice and tumors sizes. The luciferase expression, however, consistently peaked between the 17.5 and 20

minute time point intervals. Thus, 18 minutes was chosen as the peak luminescent time at which all mice tumors were henceforth imaged.

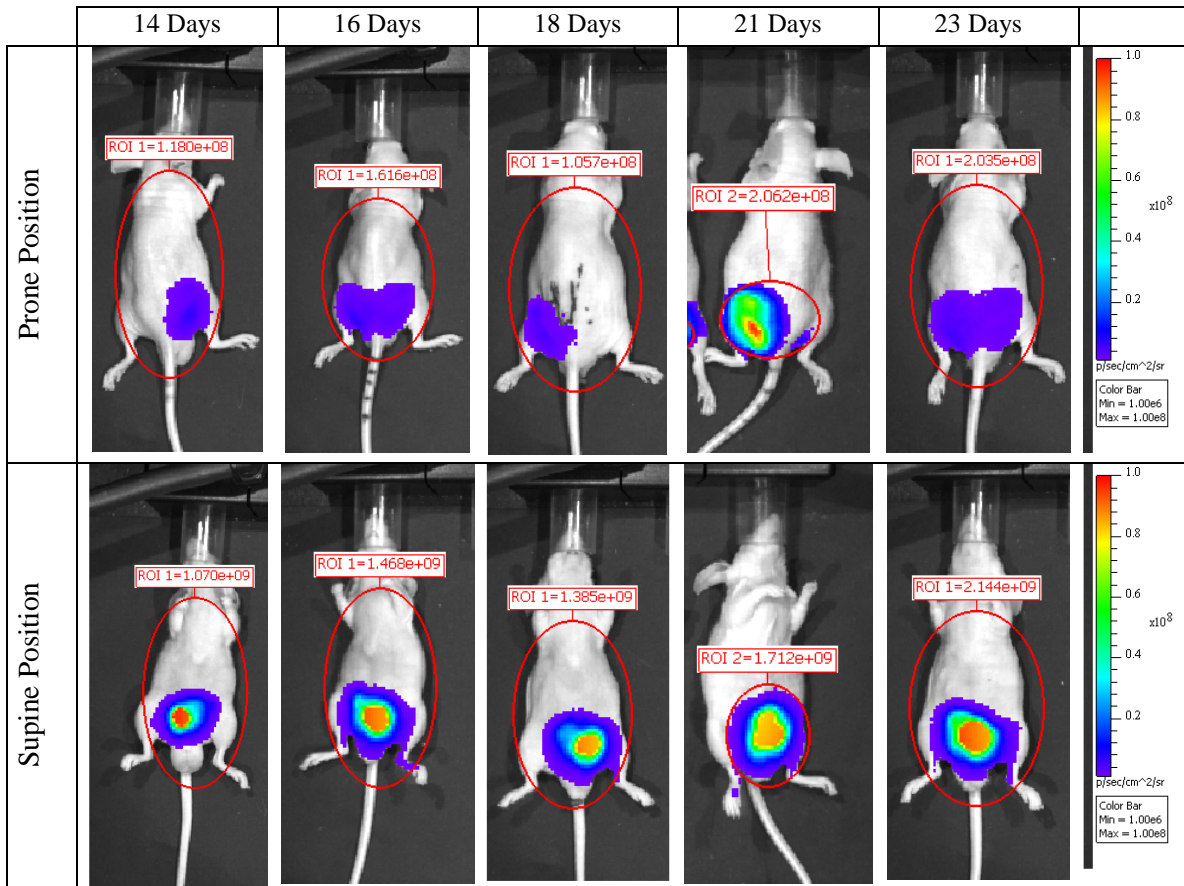
Next, the relative amount of reflected luminescence was determined by measuring the flux associated with a secondary control mice also placed in the IVIS Imager with a mouse injected with luciferin. This data can be seen in Appendix B, however, the reflected photon flux was found to range from  $7.84 \times 10^5$  to  $3.01 \times 10^6$  photons/sec for tumors grown up to 18 days. This range is important in establishing a threshold value for determining the presence of residual tumor cells inside the mouse once the primary tumor has been removed for measurement. Since the model was to incorporate mice with tumors having been grown for 30 days, the reflective threshold was established at  $1 \times 10^7$ . Any mouse with residual flux over this limit was not included in the luminescent correlation model, as enough cells remained to conclude that the measured tumor mass and volume were inaccurate.

After sacrificing mice at predetermined time points, the mass and volume of the excised tumors were then measured. These measurements led to the development of a time dependent tumor growth model for PC-3 cells xenografted orthotopically in the prostate, as depicted in Figure 2.

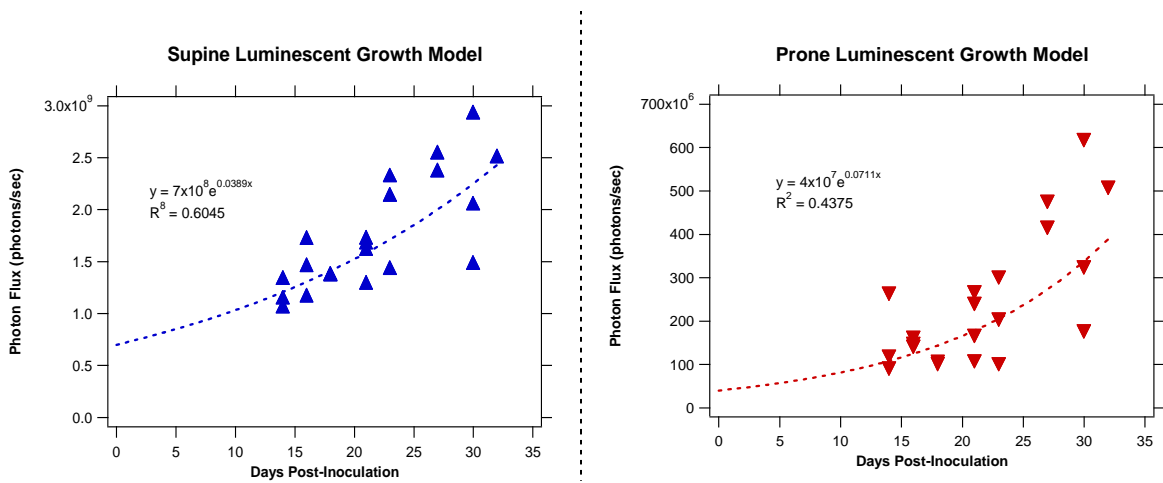


**Figure 2: Recorded prostate tumor sizes for Balb/C nude mice (n=34) after orthotopic inoculation with  $1 \times 10^6$  PC-3M-luc-C6 cells.**

While excised tumor mass provided a definitive growth model, an additional growth model was constructed that tracked tumor size relative to non-invasive luminescent imaging. Two potential imaging modalities were examined for this model by measuring quantitative photon fluxes for mice in the prone position and the supine position. Figure 3 illustrates and compares the captured IVIS luminescent images for both modalities. Figure 4 displays the quantitative growth models based on the different imaging positions.



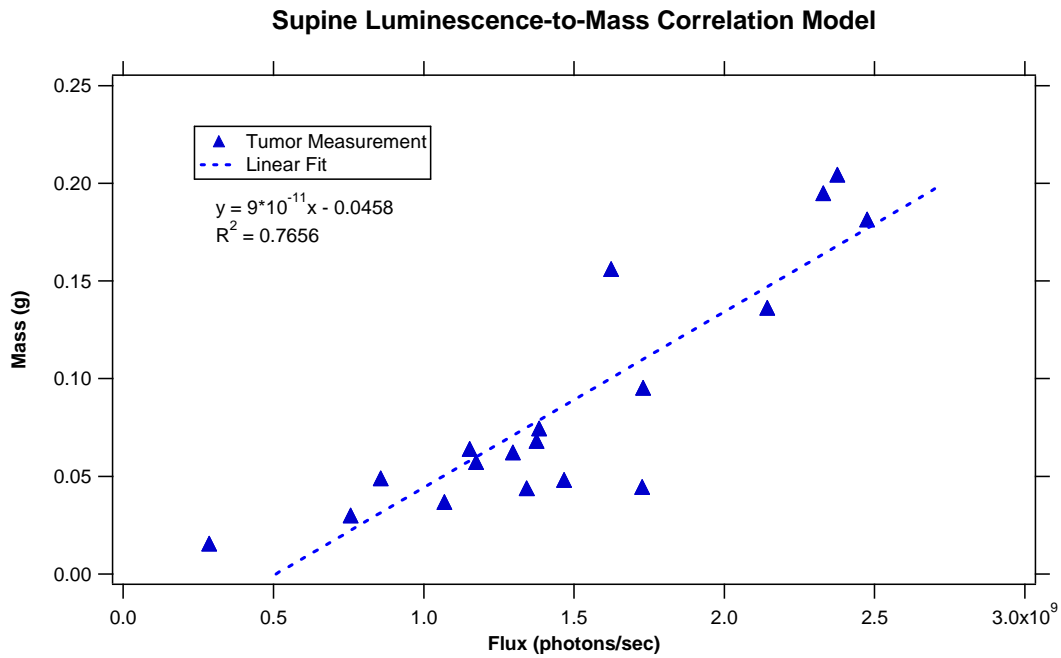
**Figure 3: Xenogen™ IVIS *in vivo* images comparing the PC-3M-luc-C6 photon flux intensity of different mice in both the prone and supine position. Each mouse was imaged and the designated time point and then sacrificed.**



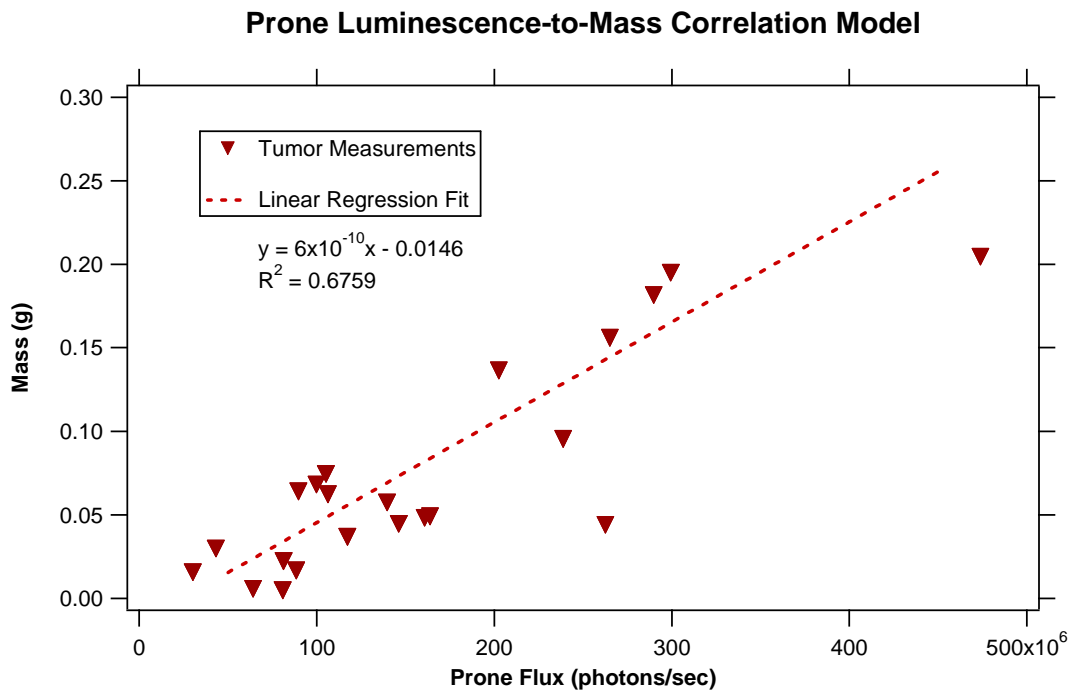
**Figure 4: Luminescent photon fluxes for n=34 mice sacrificed at different time points after inoculation with  $1 \times 10^6$  PC-3M-luc-C6 cells.**

Figure 3 and Figure 4 reveal that the measurable photon flux from the supine position is observed to be an order of magnitude larger than that measured from the prone position. In addition, the focal point of the supine luminescent intensity image appears to more accurately depict the spatial position of the prostate within the peritoneal cavity. Both luminescent signals display a generalized exponential growth behavior, but the regression lines have weak  $R^2$  values (0.6045 and 0.4375 for supine and prone respectively).

Before beginning radiotherapy, however, a correlation model between the photon flux signal of a tumor and its actual mass must be established. Mass was selected as the direct comparison method because it can be determined without regard to the particular geometry of a tumor's growth. Moreover, tumors may have to be excised in pieces, making volume measurements difficult. These two factors made mass ideal for comparing against a luminescent signal. In addition, the variability of the luminescent growth models suggested that strict criteria must be applied for data inclusion to guarantee a reliable correlation model. This was achieved by ensuring that tumors were only included if 1) the residual luminescence was under the  $1 \times 10^6$  threshold previously established and 2) the excised tumor tissue was ensured to only contain tumor tissue. The resulting supine, prone and *ex vivo* correlation models are found in Figure 5 and Figure 6.



**Figure 5: Correlation model for tumor mass as determined from luciferase luminescence measured in the supine position.**



**Figure 6: Correlation between luciferase luminescence measured in the prone position and actual tumor mass.**

As the radiotherapeutic dose is determined from the tumor volume, a second correlation was established between mass and volume. In this case, tumors were only included if 1) their geometry was regular enough to be determined accurately and 2) the volume was only compared against the mass contributing to the primary tumor shape (not necessarily all of the tumor excised from the mouse). Figure 7 shows the results.

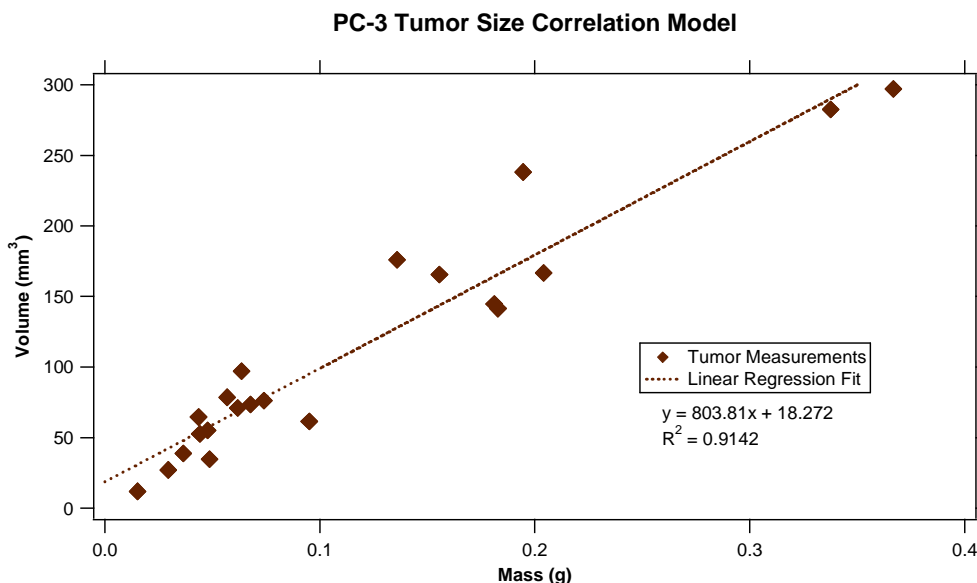
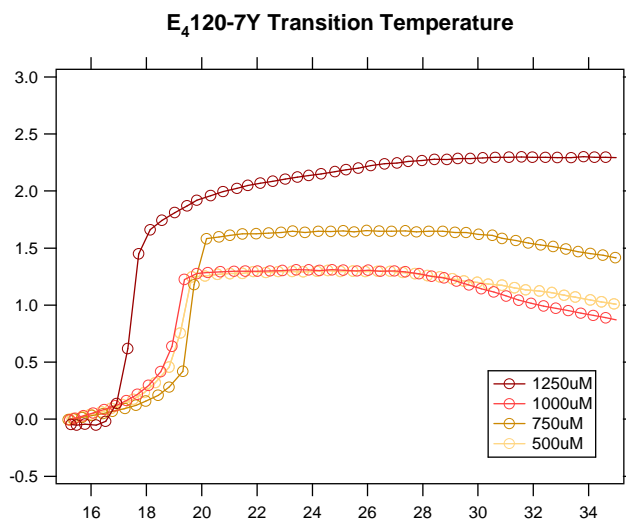


Figure 7: Model depicting the dependency of PC-3 tumor volume on its measurable mass.

### 3.2. ELP Construction and $^{131}\text{I}$ Radiolabeling

Once ELP has been properly collected and purified in sufficient quantities, the optimal ELP concentration for performing therapeutic injections was determined from an assessment of two factors. Foremost, the final injection concentration was selected based on the observed transition temperature ( $T_T$ ) of  $(\text{VPGVG})_{120}\text{-7Y}$ . As observed by Lessin and Parkes [15], mouse body temperature can vary from 28°C-38°C depending on activity, sedation or anesthesia.  $\text{E}_4\text{120-7Y}$  must therefore be formulated such that will always undergo phase transition to its coacervate form at the lowest possible mouse body temperature. Previous studies conducted by Liu, W [11] established a  $T_T$  of 20.5°C for  $\text{E}_4\text{120-7Y}$  at 1000 $\mu\text{M}$ . Spectrometer absorbance

measurements of varied concentrations, found in Figure 8 , show that all concentrations above 500 $\mu$ M exhibit a  $T_T$  between 16 $^{\circ}$ C and 21 $^{\circ}$ C, well under the 28 $^{\circ}$ C body temperature threshold. As also reported by Liu, this concentration formulation inhibited the *in vivo* degradation of the coacervate (as seen at lower concentrations) when injected intratumorally into subcutaneous, FaDu tumors on the dorsal flank of mice.



**Figure 8: Transition temperatures for E<sub>4</sub>120-7Y prepared at different concentrations**

The second major factor in determining the ELP formulation was determining the concentration that maximized ELP recovery from the purification column using size-exclusion centrifugation. The different ELP concentration and centrifuge parameters were evaluated as seen in Table 1.

**Table 1: Spin-purification recovery for different ELP concentrations**

Concentration	Initial Volume	Column	RPM	Time	% Recovered
1000 $\mu$ M	800 $\mu$ l	5ml, 40kDa	2500	4 min	33.6%
750 $\mu$ M	800 $\mu$ l	5ml, 40kDa	2500	4 min	53.8%
500 $\mu$ M	650 $\mu$ l	5ml, 40kDa	2500	4 min	92.5%
250 $\mu$ M	650 $\mu$ l	5ml, 40kDa	2500	4 min	92.5%
750 $\mu$ M	800 $\mu$ l	5ml, 40kDa	3000	6 min	56.3%
750 $\mu$ M	650 $\mu$ l	5ml, 40kDa	3000	2x 4min	81.5%
500 $\mu$ M	650 $\mu$ l	2ml, 40kDa	2500	4 min	73.8%

Initially, 750  $\mu\text{M}$  was viewed as a potential formulation due to its similar  $T_T$  to 1000  $\mu\text{M}$ . However, the percent recovery could not be raised to adequate levels. The decision was then made to formulate the ELP at 500  $\mu\text{M}$  for radiolabeling conjugation. This would ensure recovery of over 70% of  $^{131}\text{I}$ -labeled ELP. Once labeled, though, the ELP would be mixed at a 1:1 volume ratio with additional ELP prepared at 1500  $\mu\text{M}$ . The resultant ELP would maximize radioactivity recovery while having an injectable concentration of 1000  $\mu\text{M}$ , maintaining the appropriate  $T_T$  and maximizing degradation resistance. Maintaining the same therapeutic formulation as Liu [11] also would allow for cross-comparison with his subcutaneous model.

### **3.3. Radiotherapy Trials**

As of the time of publishing this thesis, the trials assessing the efficacy of the radiotherapy administered through intratumoral ELP injection are still ongoing. As such, the data in this section is preliminary. Upon completion, this section will be updated with all finalized results. Radiotherapy has been administered in 3 different groups. The first administration group consisted of only control mice to perfect handling techniques. The second group consisted of injections of ELP (mixed to 1000 $\mu\text{M}$ ) at a final radioactive concentration of 1.465 mCi / 40 $\mu\text{l}$ . This was lower than the target therapeutic dose of 2 mCi / 40 $\mu\text{l}$ , so the injection volume ratio was raised. For the third administration injection group, the ELP was labeled and diluted to the appropriate dose. 12 total mice were treated with  $^{131}\text{I}$ -ELP, while 14 mice were treated as controls with unlabeled ELP. The injection details are found in Table 2. Each mouse was monitored to determine tumor regression over time (Figure 9), intratumoral radiation levels were tracked against isotope decay (Figure 10), and mouse survival was tracked between the control and test groups (Figure 11). These results are used to determine the efficacy of the orthotopic, intratumoral radiodepot.

**Table 2: ELP injection volumes and radioactive doses administered during radiotherapy**

Mouse	Body Weight (g)	Supine Flux (photons/sec)	Tumor Volume (mm <sup>3</sup> )	Inj. ELP (μl)	<sup>131</sup> I Activity (μCi)	Term. Date
RT11	23.3	1.235x10 <sup>9</sup>	70.8	19.9	0	3/23
RT12	27.3	1.113x10 <sup>9</sup>	62.0	17.4	0	3/12
RT13	26.1	1.273x10 <sup>9</sup>	73.6	20.7	0	3/26
RT14	25.3	1.192x10 <sup>9</sup>	67.7	19.0	0	3/24
RT15	30.3	1.646 x10 <sup>9</sup>	100.5	28.3	0	3/15
RT21	25.7	1.198e x10 <sup>9</sup>	68.1	20.6	0	3/23
RT22	28.9	8.984 x10 <sup>9</sup>	631.4	13	0	3/31
RT23	24.2	5.098 x10 <sup>9</sup>	350.3	0	0	3/18
RT24	25.4	1.075 x10 <sup>9</sup>	59.2	16.6	0	3/31
RT25	25.0	2.054 x10 <sup>9</sup>	130.0	36.6	0	3/13
RT31	25.8	1.373 x10 <sup>9</sup>	80.8	22.7	0	3/15
RT32	25.8	2.004 x10 <sup>9</sup>	126.4	35.6	0	3/12
RT33	26.6	1.805 x10 <sup>9</sup>	112.0	33.8	0	3/23
RT35	23.7	3.235 x10 <sup>9</sup>	215.5	60.7	0	3/23
RT41	23.8	1.100 x10 <sup>9</sup>	61.0	32	1133	n/a
RT44	25.1	7.434 x10 <sup>8</sup>	35.2	18.4	90.6	n/a
RT45	22.5	1.905 x10 <sup>9</sup>	119.3	62	1585	3/10
RT51	20.6	9.363 x10 <sup>8</sup>	49.2	14	457	n/a
RT52	21.2	1.395 x10 <sup>9</sup>	82.4	28	1367	n/a
RT53	14.1	6.061 x10 <sup>8</sup>	25.3	13	212	n/a
RT54	22.0	1.640 x10 <sup>9</sup>	100.1	55	2560	3/5
RT55	27.1	4.804 x10 <sup>8</sup>	16.2	6	118	n/a
RT61	25.7	2.069 x10 <sup>9</sup>	131.1	103	2360	n/a
RT62	18.5	1.364 x10 <sup>9</sup>	80.1	31	1538	3/2
RT63	20.4	1.625 x10 <sup>9</sup>	99.0	45	2260	n/a
RT64	22.3	1.649 x10 <sup>9</sup>	100.8	53	1270	3/8

### Average *In Vivo* Radioactivity Post-Administration

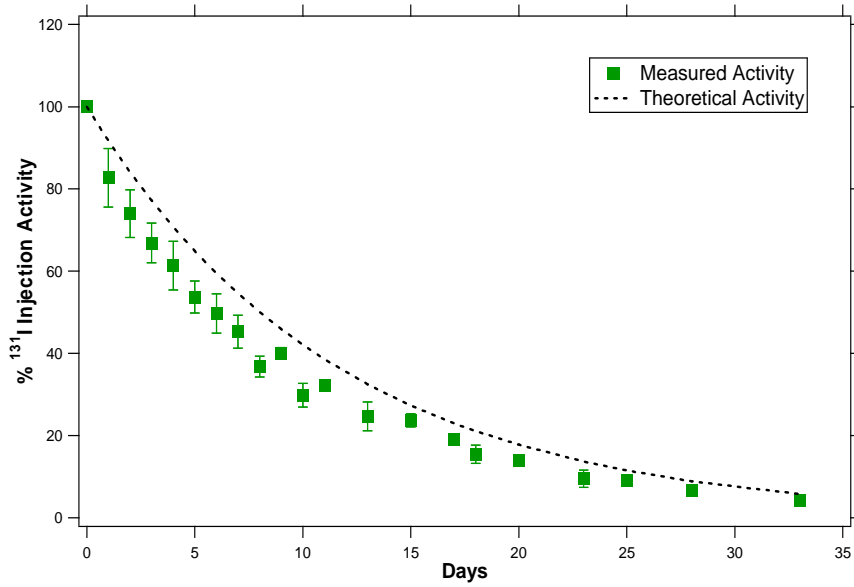


Figure 9: Intratumoral radiation level measured over time and compared against the theoretical decay behavior for <sup>131</sup>I.

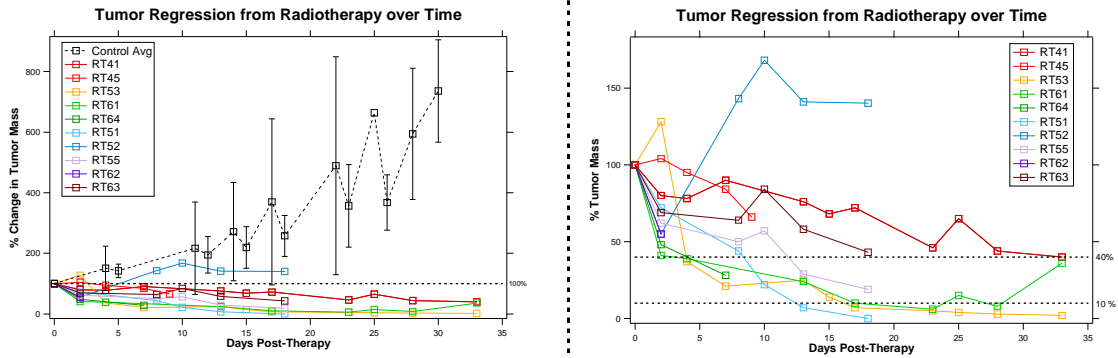
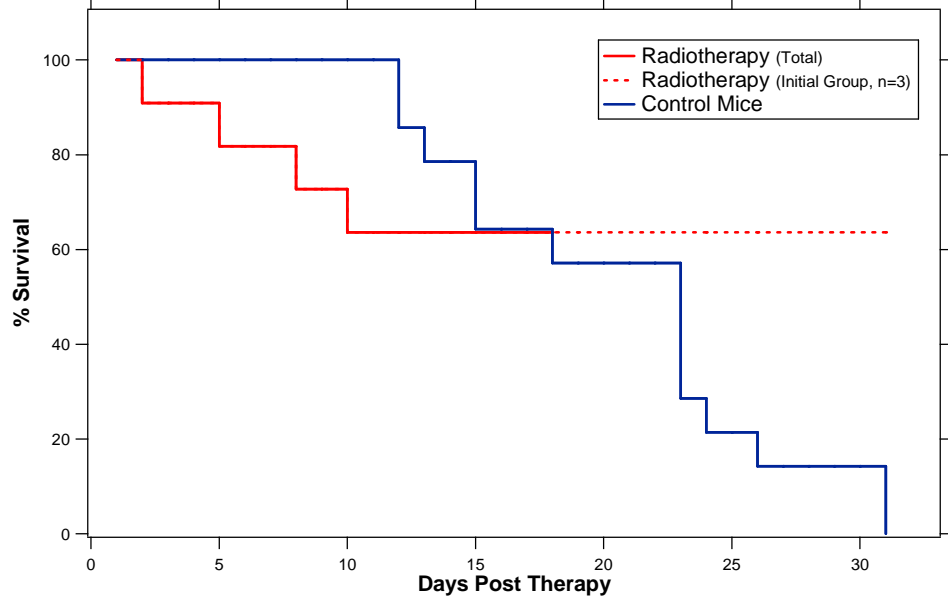


Figure 10: Tumor regression in mice resulting from intratumoral radiotherapy

### Survival Rates following Radiotherapy Injection (still on-going)



**Figure 11: Survival chart comparing mice having received radiotherapy (n=12) against those that received control injections of unlabeled E<sub>4</sub>120-7Y (n=14).**

## 4. Discussion

### 4.1. *Orthotopic Tumor Growth Model*

Establishing an accurate and reliable correlation model for determining PC-3 tumor size in a non-invasive manner was critically important to this experiment. By successfully correlating bioluminescent activity to tumor size and volume, tumor regression in response to treatment could henceforth be tracked without sacrificing the mouse. While stringent criteria limited which tumor growth data points were used for developing the correlation model (Figure 5), the resulting model showed reasonably strong fit characteristics having a  $R^2$  value of 0.7656. While this provided a predictive model that was good enough for determining tumor volume to plan therapy doses, it was still not completely accurate.

There are several reasons for the observed inaccuracy in such a model. First, as described in Yu [14], the amount of luciferase expressed in each PC-3 cell varies. This causes cell to cell variation in the maximal photon flux a tumor cell might exhibit when administered luciferin. Second, the ability to accurately and completely excise tumor cells from non-cancerous tissue by the naked eye is highly difficult. While it was previously discussed that tumor mass provided the best means for correlating tumor size and luminescent intensity, it was still subject to error arising from the surgical precision used when excising the tumor. The use of residual flux comparison helped ensure that all tumor cells were harvest and weighed in connection with a signal. The converse problem was that sometimes healthy tissue was indifferntiable to the naked eye from tumor tissue artificially raised the measured mass of the tumor. This was issue was particularly relevant for the inclusion of bladders that exhibited partial tumor cell growth in the bladder membrane.

A third issue that confounded attempts at establishing a more accurate model can be ascertained by comparing the prone and supine flux images. Measurements taken in the prone

position demonstrated remarkably lower intensities than those in the supine position. The reason for this is the photon flux from the tumor cells must penetrate through a much greater amount of tissue to reach the photon sensitive camera. The tissue serves to both absorb and scatter the photons, attenuating the signal's intensity. By taking images in the supine position helps limit tissue attenuation of the signal, the relative position of the prostate within the mouse could not be controlled. Dissection procedures showed that some tumors resided very close to the surface of the abdomen, while others were further recessed inside the peritoneal cavity and covered by tissues such as the seminal vesicles, fatty tissues or preputial gland. Such an issue is uncontrollable for non-invasive imaging, but still serves to introduce error into model.

The final complicating factor arises from the ever increasing size of the tumor in the model. As the tumor becomes more massive, it becomes more difficult for luciferin to be transported equally to all PC-3 cells. Several factors affect this, such as tumor vascularization and a high intratumoral pressure, may cause a percentage of cells to remain luminescently dormant despite *i.p.* administration of luciferin. As seen in Figure 1, the ability to capture the peak luminescence exhibits a greater sensitivity to time dependence. This arises from the fact that the luciferin injection formula is based off a mouse's body weight. Smaller tumors are substantially saturated by luciferin, allowing them to remain at peak intensity longer. Larger tumors though, receiving the same volume of luciferin based on the mouse's weight, will consume the luciferin more readily and thus exhibit sharper peaks. To improve upon this flaw in future studies, one could adjust the luciferin injection formula to incorporate the exponential growth a tumor exhibits over time from Figure 2. This modification would ensure that all tumors are equally saturated by luciferin during images, regardless of size.

Despite the flaws inherent to the luminescent model herein developed, the luminescence correlation to tumor growth provides a reasonably reliable model for determining and tracking the

prostate tumor size in a non-invasive manner. By comparing the different imaging modalities, it is quickly apparent that the supine position provides a better method for measuring luminescent flux. By coupling it with the correlation between a tumor's mass and volume, the following formula and relative error:

$$Vol_{PC3} = 7.234 \times 10^{-9} * \text{Supine Flux} - 18.54$$

Error ~ 21.7%

## **4.2. Radiotherapy Trials**

Use of E<sub>4</sub>120-7Y as an intratumoral <sup>131</sup>I radio depot has provided mixed results to date. Following administration, mice typically experience a 10% loss in body weight and exhibit lethargic behavior. Examination of the intratumoral radioactivity levels against the theoretical decay of <sup>131</sup>I indicates that the ELP coacervate remains relatively stable as long as 20 days and resists degradation within the tumor site. This is important for verifying that the majority of the conjugated radionuclide is actively contributing to the treatment of the prostate cancer. This helps to minimize the initial radioactive dose since the ELP is not being degraded and cleared by the body within the therapeutic time window. Even more promising the data in Figure 10 shows clear arrestment and regression of the prostatic tumor. In fact, most tumors treated to date have shown progression that indicates a 40% - 60% reduction in tumor size within one week of intratumoral injection. When comparing the therapeutic regression against the rampant tumor growth observed for the control mice, it is abundantly clear that the ELP is working effectively as an intratumoral radiodepot.

Unfortunately, the survivability results have not been as positive. Of the 12 mice having received radiotherapeutic injections, 4 of them have died within one week of treatment. One mouse had to be sacrificed due to excessive body weight loss. The cause of death for the other 3

could not be determined their corpses were partially cannibalized by the other mice they were caged with. In each case though, weight loss was not of concern prior the day prior. Considering that control mice lived, on average, 21 days after their sham injections, tumor burden and metastasis formation can most likely be ruled out. Instead, I would hypothesize that the radioactivity of the ELP depot most likely damaged vital urogenital organs (such as the urethra or bladder), which most likely led to renal failure and death.

Unlike previous studies conducted on a subcutaneous dorsal flank model, the orthotopic model consists of vital organs in close vicinity with the radiodepot. While the ELP depot is injected into the central core of the tumor, the strength of the dose might have lead to incident radiation damaging peripheral tissue. Thus, subsequent trials should examine determining a maximal tolerable dose for radiation treatment administered orthotopically to the prostate. The dose can then be tuned to retain its effectiveness in tumor regression while eliminating mortality due to over irradiation of other organs. A second potential solution would be to consider using a different radioactive nuclide whose beta emissions has slightly less energy than  $^{131}\text{I}$ . By selecting lower energy beta emitters, the radiation from the depot would have a shorter tissue penetration. This would reduce the amount of radiation that non-cancerous tissue was exposed to. Table 3 shows a list of potential radionuclides that are currently accepted in clinical radiotherapy applications. For brachytherapy, only beta emitters that undergo 100%  $\beta^-$  decay are considered due to the stability of their decay products and maximal therapeutic radiation. Further examination of *in vivo* toxicity characteristics for the isotopes would require examination before further therapy could be conducted. However, isotopes with half-lives of 5-14 days would be optimal for intratumoral depot delivery. Finally, additional trials could also explore administering the effective treatment with multiple injections to different spatial hemispheres of

the prostate tumor. This approach could help to ensure that the core of the radiodepot is located further away from the urethra and other vital organs.

**Table 3: Activity Information for Clinically Accepted Beta-Emission Radioisotopes**

<b>Isotope</b>	<b>Half-life</b>	<b>Average Beta Emission (keV)</b>	<b>Range of Beta Emissions (keV)</b>	<b>Decay Product</b>
<sup>131</sup> I	8.02 days	577.96	247.9-806.9	<sup>131</sup> Xe
<sup>177</sup> Lu	6.73 days	450.9	177.0-498.3	<sup>177</sup> Hf
<sup>188</sup> W	69.4 days	346.4	58-349	<sup>188</sup> Re
<sup>182</sup> Ta	114.4 days	431.83	261.1-1714.2	<sup>182</sup> W
<sup>60</sup> Co	5.27 years	319.61	318.2-1491.4	<sup>60</sup> Ni
<sup>192</sup> Ir	73.8 days	437.56	53.5-675.1	<sup>192</sup> Pt
<sup>47</sup> Sc	3.35 days	491.3	440.9-600.3	<sup>47</sup> Sc
<sup>67</sup> Cu	2.58 days	432.19	168.2-561.7	<sup>67</sup> Zn

As the study continues, further study will be required for several factors. First, mice will require long term observation to determine if treatment groups experience complete tumor regression, partial tumor regression or tumor recurrence. If only partial regression is achieved, the percent reduction must be examined as a potential adjuvant therapy that enhances the probability of success with radical prostatectomy. Second, surviving mice will need to be examined to discover whether the healthy tissue recovery is achieved in the affected dorsolateral prostate lobe. Histological studies of tissue necrosis and recover for both the prostate and peripheral organs will need to be conducted to verify the effects of radiation. Third, a biodistribution study needs to be performed to affirm accumulation of radioactive iodine in other organs once the ELP has been cleared. Finally, further experimentation should be done to evaluate the volume ratio of ELP require to inject intratumorally. The current ELP to tumor volume ratio of 26.7% might not best homogenize the radioactivity experienced by all regions of the tumor. Further intratumoral diffusion and penetration studies might help to optimize the spatial delivery of radionuclides within the prostate tumor

## 5. Conclusions

The results of this study have successfully established a readily reliable and accurate model for non-invasively measuring prostatic tumor growth. Further improvements to the procedure could provide slight improvements to the model developed within; however uncontrollable methodology limitations and histological variance between individual mice will ultimately limit the degree of improvement that can be obtained. For the purposes of developing a method to determine *in vivo* tumor size for monitoring regression in an orthotopic nude mouse, the model was sufficient.

The on-going study of using ELP as a radionuclide conjugate for intratumoral depot delivery requires further investigation at this time. Similar to previous studies on subcutaneous models, preliminary results have shown its effectiveness in achieving tumor regression in treated mice. However, early survivability rates in the orthotopic model suggest that the current radioactivity formulation is too high. The sensitivity of the prostate anatomy and surrounding organs necessitate a more moderate approach for radioactive treatment.

## Appendix A: (VPGVG)<sub>120</sub>-Y<sub>7</sub> Design by Liu et al.

In a previous set of experimental trials conducted by the Chilkoti Group at Duke University, Liu et al. optimized the synthetic ELP (VPGVG)<sub>n</sub> for use as an intratumoral coacervate depot by tuning the molecular weight, concentration and attaching a number of carboxyl-terminus tyrosine residues of the molecule. Experimental results, shown in Figure 12, demonstrated that increasing the molecular weight of the polypeptide heightened the 1 week retention until a ceiling of 50 kDa (n=120 repeats) was reached. The higher molecular weight also lowered the observed transition temperature. However, molecular weights above 50kDa showed no appreciable improvements in tumor retention to justify the significantly larger molecule.

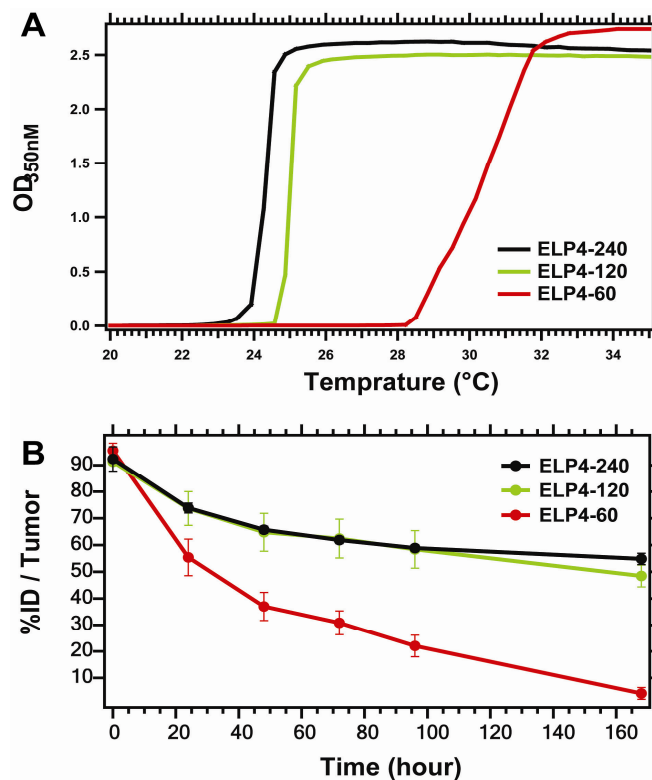
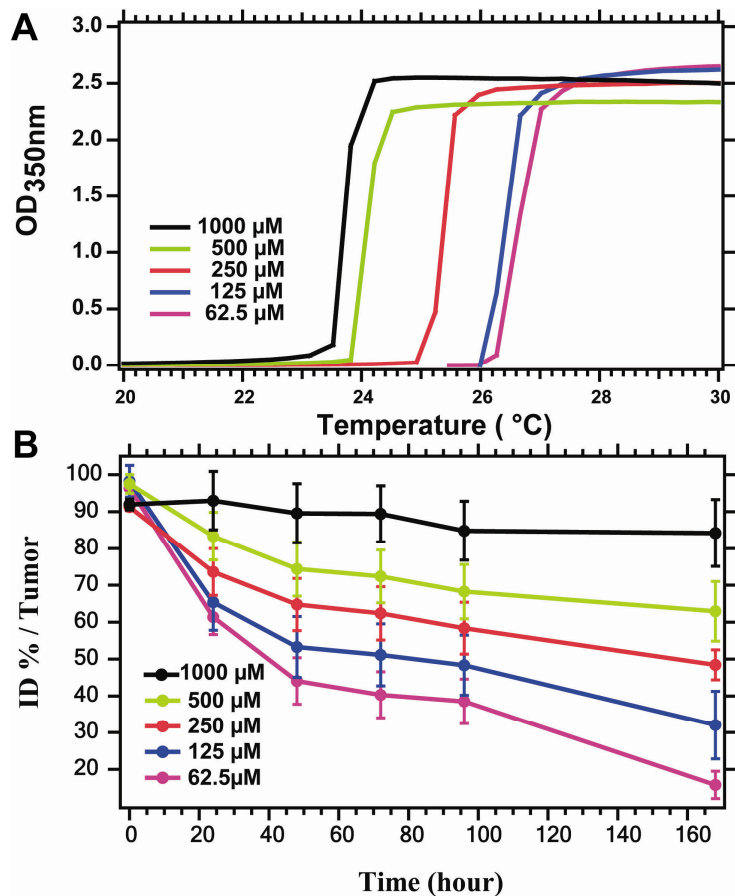


Figure 12: (A) Turbidity profile displaying the phase transition profile for ELP molecules (containing a V residue) varying in pentapeptide repeat length. (B) Percent of ELP depot retained intratumorally over time.

In a similar fashion, a spectrum of ELP concentrations were characterized using turbidity phase transition tests and injected subcutaneously to monitor intratumoral degradation. The results in Figure 13 show that raising the concentration to 1000  $\mu\text{M}$  increased the 1-week intratumoral retention percentage to 85% while lowering the  $T_i$  to 23.5°C. Lower concentrations tended to reduce the performance of the ELP depot in both regards.



**Figure 13: (A) Transition temperature of ELP (VPGVG)<sub>120</sub> as determined over varying concentrations by measuring relative absorbance at 350nm. (B) 1-week intratumoral retention performance of ELP depots formulated at varying concentrations**

Finally, the effects of adding the carboxyl-terminus tail composed of tyrosine residues of various lengths was explored. The tyrosine tail served 2 functional purposes: providing a conjugation site for the <sup>131</sup>I radionuclide and improving the intratumoral retention by increasing

the hydrophobicity of the overall polypeptide. By examining multiple tyrosine residues of length 1, 4 and 7 in Figure 14, it was found that a 7 tyrosine tail exhibited the best intratumoral resistance to degradation during the course of therapeutic administration. It also lowered the  $T_1$  to  $\sim 21.5^\circ\text{C}$ , improving the coacervate transition characteristic for *in vivo* administration.

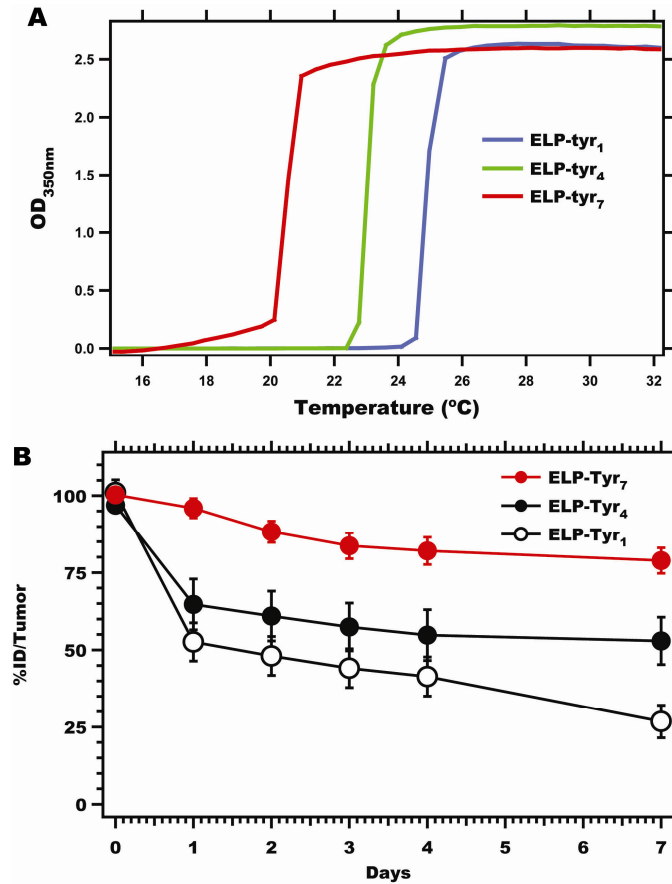


**Figure 14: (A) Transition temperatures of the ELP construct (VPGVG)<sub>120</sub> @ 1000 μM with varying number of carboxyl-terminus tyrosine residues. (B) Intratumoral retention performance of varying tyrosine tail lengths.**

## Appendix B: Orthotopic PC-3 Growth Model Data

**Table 4: Individual tumor sizes, both in terms of mass and volume, for mice inoculated with  $1 \times 10^6$  PC-3 cells and grown for a pre-determined number of days**

Mouse	Inoculation Date	Sacrifice Date	Term Days	Tumor Mass (g)	Tumor Volume (mm <sup>3</sup> )
12	24-Oct	7-Nov	14	0.0366	38.67
13	24-Oct	7-Nov	14	0.0437	64.36
14	24-Oct	7-Nov	14	0.0637	96.95
15	31-Oct	16-Nov	16	0.0480	54.90
21	31-Oct	16-Nov	16	0.0443	52.33
22	31-Oct	16-Nov	16	0.0154	11.69
24	31-Oct	16-Nov	16	0.0571	78.37
34	11-Nov	29-Nov	18	0.0679	73.40
35	11-Nov	29-Nov	18	0.0296	26.93
41	11-Nov	29-Nov	18	0.0742	75.88
44	11-Nov	2-Dec	21	0.0620	70.77
124	3-Aug	24-Aug	21	0.0488	34.45
125	3-Aug	24-Aug	21	0.0952	61.20
153	25-Aug	15-Sep	21	0.1558	165.20
165	6-Sep	27-Sep	21	0.1813	144.58
31	31-Oct	23-Nov	23	0.1947	237.99
32	31-Oct	23-Nov	23	0.1361	175.80
54	25-Jan	21-Feb	27	0.3669	296.81
55	25-Jan	21-Feb	27	0.2043	166.38
61	25-Jan	24-Feb	30	0.1830	141.14
62	25-Jan	26-Feb	32	0.3378	282.34

## Appendix C: Orthotopic Flux Correlation Data

**Table 5: Luminescent flux measurements for sacrificed mice, measured in different postures, and the corresponding tumor size.**

Mouse	Term Days	Tumor Mass (g)	Prone Flux (p/s/cm <sup>2</sup> /sr)	Supine Flux (p/s/cm <sup>2</sup> /sr)	Residual Flux (p/s/cm <sup>2</sup> /sr)
12	14	0.0366	1.175E+08	1.070E+09	3.371E+06
13	14	0.0437	2.628E+08	1.344E+09	5.582E+06
14	14	0.0637	8.998E+07	1.154E+09	7.616E+06
15	16	0.0480	1.610E+08	1.468E+09	6.008E+06
21	16	0.0443	1.464E+08	1.728E+09	5.772E+06
22	16	0.0154	3.041E+07	2.876E+08	1.790E+06
24	16	0.0571	1.398E+08	1.175E+09	6.838E+06
34	18	0.0679	1.002E+08	1.377E+09	2.109E+06
35	18	0.0296	4.339E+07	7.585E+08	3.925E+06
41	18	0.0742	1.054E+08	1.385E+09	9.717E+06
44	21	0.0620	1.065E+08	1.298E+09	2.861E+06
124	21	0.0488	1.640E+08	8.742E+08	N/A
125	21	0.0952	2.390E+08	1.747E+09	6.763E+06
153	21	0.1558	2.653E+08	1.624E+09	5.174E+06
165	21	0.1813	2.901E+08	2.476E+09	N/A
31	23	0.1947	2.996E+08	2.330E+09	7.261E+06
32	23	0.1361	2.029E+08	2.144E+09	7.429E+06
54	27	0.3669	4.141E+08	2.551E+09	5.517E+06
55	27	0.2043	4.741E+08	2.377E+09	9.560E+06
61	30	0.1830	1.755E+08	1.488E+09	6.593E+06
62	32	0.3378	5.068E+08	2.513E+09	3.839E+06

## References

1. American Cancer Society, Inc. (2010). "Cancer Statistics 2010". [www.cancer.org](http://www.cancer.org)
2. Huggins C, Scott W, Heinen JH (1942). "Chemical Composition of Human Semen and of the Secretions of the Prostate and Seminal Vesicles." *American Journal of Physiology*. **136**, 3:467-473
3. National Kidney & Urologic Diseases Information Clearinghouse, NIH (2010). "Prostate Enlargement: Benign Prostatic Hyperplasia." <http://kidney.niddk.nih.gov>.
4. Tai, S, Huang J et al. (2011). "PC3 is a Cell Line Characteristic of Prostatic Small Cell Carcinoma." *The Prostate*. **71**, 1668-1679.
5. Sahgal A, Roach M (2007). "Permanent Prostate Seed Brachytherapy: A Current Perspective on the Evolution of the Technique and its Application." *Nature Clinical Practice: Urology*. **4**, 12:658-670.
6. Saito S, Yorozu A et al. (2007). "Brachytherapy with Permanent Seed Implantation." *International Journal of Clinical Oncology*. **12**, 395-407.
7. McDaniel J, Callahan D, Chilkoti A. (2010). "Drug Delivery to Solid Tumors by Elastin-like Polypeptides." *Advanced Drug Delivery Reviews*. **62**, 1456-1467.
8. Liu W, MacKay A, Dreher M, Chen M, McDaniel J, Simnick A, Callahan D, Zalutsky M, Chilkoti, A (2010). "Injectable intratumoral depot of thermally responsive polypeptide-radionuclide conjugates delays tumor progression in a mouse model." *Journal of Controlled Release*. **144**, 2-9.
9. Rodriguez-Cabello JC (2004). "Smart Elastin-like Polymers." *Advances in Experimental Medicine and Biology*. **553**, 45-57.
10. Shamji MF, Betre H, Kraus VB, Chen, J, Chilkoti A, Pichika R, Masuda K, Setton LA (2007). "Development and characterization of a fusion protein between thermally responsive elastin-like polypeptide and interleukin-1 receptor antagonist: sustained release of a local anti-inflammatory therapeutic." *Arthritis & Rheumatism*. **56**, 11:3650-3661.
11. Liu W, McDaniel J, Li X, Asai D, Quiroz F, Schaal J, Park JS, Zalutsky M, Chilkoti A (2012). "Development of an Alternative Local Radionuclide Delivery Depot to Brachytherapy Using Thermally-Responsive Protein-Polymer." *Unpublished*.
12. Price D (1963). "Comparative aspects of development and structure in the prostate". *Monogr. Natl. Cancer Inst.* **12**, 2-15.
13. Kaighn ME, Narayan KX, Ohnuki Y, Lechner JF, Jones LW (1979). "Establishment and characterization of a human prostate carcinoma cell line (PC-3)". *Invest Urol*. **17**, 16-23.
14. Yu SF, Jenkins D, Bishop J (2008). "Bioware Cell Line PC-3M-luc-C6", *Caliper Life Science*. 1-4.
15. Lessin AW, Parkes MW (1957). "The Relation Between Sedation and Body Temperature in the Mouse". *Brit. Journal of Pharmacology*. **12**, 245-250